User Attraction via Wireless Charging in Downlink Cellular Networks

Jeemin Kim, Jihong Park, Seung-Woo Ko, and Seong-Lyun Kim
School of Electrical and Electronic Engineering, Yonsei University
50 Yonsei-Ro, Seodaemun-Gu, Seoul 120-749, Korea
Email: {jmkim, jhpark.james, swko, slkim}@ramo.yonsei.ac.kr

***Abstract*—A strong motivation of charging depleted battery can be an enabler for network capacity increase. In this light we propose a spatial attraction cellular network (SAN) consisting of macro cells overlaid with small cell base stations that wirelessly charge user batteries. Such a network makes battery depleting users move toward the vicinity of small cell base stations. With a fine adjustment of charging power, this user spatial attraction (SA) improves in spectral efficiency as well as load balancing. We jointly optimize both enhancements thanks to SA, and derive the corresponding optimal charging power in a closed form by using a stochastic geometric approach.**

***Index Terms*—Wireless power transfer, spatial attraction, spectral efficiency, load balancing, rate coverage, stochastic geometry.**

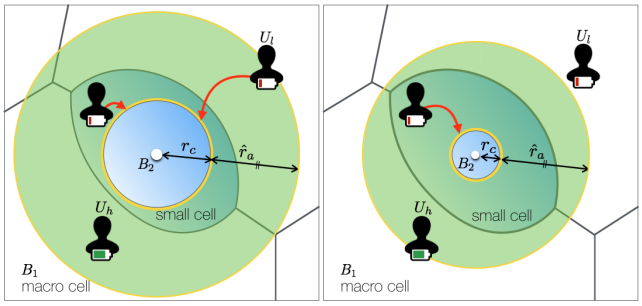

(a) High charging power (large r_c)(b) Low charging power (small r_c)

Fig. 1. Illustration of an SAN for different charging powers (or charging range r_c) with the maximum SA distance $\hat{r}_a$. A small cell BS B_2 spatially attracts battery depleting users U_ℓ to its charging rim (yellow thick circle).

I. Introduction

With the mobile data traffic explosion, the small cell network has come to the fore to offload over-utilized macro cell traffic. However, a small cell base station (BS) frequently serves a limited number of users due to its small coverage area [1], [2]. In addition, the mobility of users even make the time spent in small cell area relatively short. This results in under-utilization of small cell resources [2], motivating us to balance traffic between macro and small cells.

As a remedy for this, we suggest to enable small cell BSs to charge mobile devices wirelessly, given strong desire of mobile users to charge their devices [3]. Seeking for charging depleted batteries even makes users move to a nearby place providing power outlets [4], [5]. Therefore, a wireless power transfer (WPT) in small cell BSs can act as an incentive to yield the spatial attraction (SA) of users in macro cells toward the vicinity of small cell BSs. Throughout this paper, we call this network a spatial attraction cellular network (SAN) and its attraction amount is determined by the charging power.

The physical displacement from macro to small cells can be utilized for the improvement in macro-to-small cell *load balancing*. From the small cell users perspective who were already in the small cell coverage (see Fig. 1), this attraction also leads to the improvement in *spectral efficiency*. This is because the attraction toward their associated BSs not only increases their received powers of the desired signals but also coincidentally decreases interference.

In an SAN, these load balanging and spectral efficiency improvements vary with charging power, but their corresponding behaviors are non-trivial. From the load balanging perspective, increasing charging power for instance may incur too much associations at small cell BSs. To mitigate such an issue, it requires an optimal charging power that balances the associations between macro and small cell BSs. From the spectral efficiency perspective, on the contrary, high charging power increases the SA users' distances from the associated small cell BSs, at which the charged powers are still satisfactory in that distance (compare (a) and (b) in Fig. 1). As a result, increasing charging power decreases spectral efficiency improvement. In this paper we thus provide the SAN rate maximizing charging power that jointly optimize the load balanging and spectral efficiency improvements.

Feasibility of SAN – SAN implementation hinges on whether SA is viable in practice. Although mobile device proliferation is relentless, improving battery capacity has still been a major technical bottleneck [6]. It makes users more prone to be in danger of battery depletion, leading to a strong battery charging motivation in reality [3]. Such a motivation results in SA toward charging places, for example, when

determining where to go for coffee [4], [7] or even when charging is the sole reason for movements [5].

Another key enabler is to implement WPT capable small cells. By means of the advanced signal processing technologies such as an adaptive beamforming, microwave WPT has a potential to provide battery charging for most of small cell coverages while guaranteeing user safety [8]. When utilizing a beamforming antenna having an aperture of 3 m in radius, for instance, it theoretically yields charging at the distance of 10 meters with the charging amount of 0.5 Watt when the transmit power is 50 Watt [8].

Related Works – WPT aided cellular networks have recently attracted attention, accompanied by rapid advancement in WPT technologies [9], [10]. Its advantage in network capacity perspective has been explored in [11], [12]. The network capacity enhancement comes from allowing more communicating users in that WPT mitigates battery depletion. Along with such improvement, we also capture the network capacity increment via increasing spectral efficiency owing to SA. The SA also provides improvement via macro-to-small cell load balancing without degrading spectral efficiency. It is unlike preceding schemes such as cell range expansion (CRE) [13], [14] that balance the load in return for the spectral efficiency decrement. In detail, offloaded users in CRE are associated with small BSs who give lower signal power than the originally associated macro BSs. Than the originally associated BSs turn into dominant interferers, whose powers are even higher than the recived signal powers, leading to the decrement in spectral efficiency.

Contributions – This study examines the ramifications of WPT in downlink small cells in terms of maximizing rate-coverage, the proability of a typical user achieving data rate greater than a threshold. The main contributions are listed below.

- We propose an SAN that spatially attracts users to small cell BSs by the aid of battery charging WPT and thereby elevates the rate coverage of the network. We use a stochastic geometric approach to derive its rate coverage and demonstrate that significant improvements are feasible only with short SA distance, e.g. 125 % rate coverage when maximum SA distance is only 1 m (see Propositions 1 and 2 as well as Fig. 3 in Section III).
- An optimal charging power is derived in a closed form in an asymptotic case where user density is much higher than that of BSs such as an urban area, providing a design guideline of SAN (see Corollary 1 in Section III).
- To analyze SAN rate coverate, we consider data usage pattern dependent on user's residual energy. The analytic result shows that the more users' downlink (DL) usages are affected by their residual energies, the more rate coverage SAN can achieve (see Fig. 4).

TABLE I
SUMMARY OF NOTATIONS

Notation	Meaning
U_ℓ (or U_h)	Low (or high) battery level user
B_k	k-th tier base station for $k \in \{1, 2\}$
Φ_k (or Φ_u)	B_k (or user) locations
λ_k (or λ_u)	B_k (or user) density
P_k	B_k's information transmission power
P_{tc} (or P_{rc})	Charging transmission (or reception) power
P_u	User energy consumption during a unit time slot
r_c	Maximum charging range to charge P_u
r_a (or $\hat{r}_a$)	User spatial attraction (or maximum) distance
$\mathcal{R}_k^\ell$ (or $\mathcal{R}_k^h$)	Rate coverage of a low (or high) battery user when associated with k-th tier base station
$\mathcal{R}$	Average rate coverage of user

II. SAN System Model

A. Information Transmission

Consider a two-tier downlink cellular network comprising macro BSs B_1 and small BSs B_2. Let the subscript $k \in \{1, 2\}$ hereafter denote the corresponding tier. The k-th tier BS coordinates Φ_k follow a homogeneous Poisson point process (HPPP) with density λ_k where Φ_1 and Φ_2 are independent of each other. User locations Φ_{u} also follow a HPPP with density λ_{u}, independent of Φ_1 and Φ_2. For simplicity without loss of generality, we consider a unity time slot between the realizations of the spatial locations. All notations are summarized in Table I.

A BS in the k-th tier B_k transmits a downlink information signal with power P_k. The transmitted signal experiences path loss attenuation with the exponent $\alpha > 2$ and Rayleigh fading with unity mean. Both B_1 and B_2 utilize the same frequency, of the bandwidth W, yielding in inter-tier interference. Consider an interference-limited environment. By using Slyvnak's theorem [15], the signal-to-interference ratio (SIR) at a typical user associated with a B_k and located at the origin is given as

$$\mathsf{SIR}_k := \frac{P_k h_k^{(0)} \left|B_k^{(0)}\right|^{-\alpha}}{\sum_{j=1}^{2} \sum_{B_j^{(i)} \in \Phi_j} P_j h_j^{(i)} \left|B_j^{(i)}\right|^{-\alpha}} \tag{1}$$

where $B_k^{(0)}$ denotes the coordinates of the BS associated with the typical user, $B_k^{(i)}$ for $i \in \{1, 2, \cdots\}$ the i-th nearest interfering BS coordinates from the typical user, and $h_k^{(0)}$ and $h_k^{(i)}$ the corresponding channel fading gains independently following exponential distribution with unity mean. The notation $|\cdot|$ indicates the Euclidian norm. Multiple users in a BS are served according to a uniformly random scheduler [16].

B. User Energy Consumption

Users download information with probability u. Each information reception consumes energy amount P_u per unity time slot. For a user with residual energy amount L, it allows at most i times consecutive information receptions

when $iP_u \leq L < (i+1)P_u$ for an integer $i \geq 0$. We discretize L into L_i's according to the maximum number of information receptions i in a way that $i = \lfloor \frac{L}{P_u} \rfloor$ where $\lfloor \cdot \rfloor$ is a floor function. For more clarity without loss of generality, we consider battery capacity is $3P_u$, i.e. $L \in \{L_0, L_1, L_2, L_3\}$.

Battery depleting users are assumed to attempt less frequent information receptions. This leads to specify the information download probability u as

$$u = \begin{cases} 0 & \text{if } L \in L_0 \text{ (Empty)} \\ u_\ell & \text{if } L \in L_1 \text{ (Low)} \\ u_h & \text{if } L \in \{L_2, L_3\} \text{ (High)} \end{cases} \tag{2}$$

where $u_h \geq u_\ell \geq 0$. For notational brevity, let U_ℓ denotes battery depleting users whose residual battery energy $L \in L_1$. Similarly, U_h indicates the users having $L \in \{L_2, L_3\}$.

C. WPT Charging

Small cell BS B_2's are equipped with additional beamforming antennas dedicated for charging battery via microwave WPT. For charging battery, each user has an antenna which is associated with one of the predefined antenna patterns so that the main lobe point heads for her. Each B_2 transmits a charging signal with power P_{tc} through a power transfer dedicated frequency whose bandwidth is assumed to be unity without loss of generality. The charging channel is separated, yielding no mutual interference. The transmitted charging signal experiences path loss attenuation with the exponent $\beta > 2$. Users associate with the nearest B_2. The received charging power is

$$P_{\text{rc}} := G_m P_{\text{tc}} \max\left\{ \left| B_2^{(0)} \right|, 1 \right\}^{-\beta}, \tag{3}$$

where G_m denotes the main lobe gain. By means of highly sophisticated beamforming technique, the charging power received from non-associated B_2's is assumed to be negligibly small. For more brevity, we henceforth consider P_{tc} is normalized by P_u and always bigger than P_u. Since residual battery level is elevated when $P_{\text{rc}} \geq P_u$, the maximum charging range r_c becomes $(P_{\text{tc}}/P_u)^{1/\beta}$ which makes P_{rc} be equivalent to P_u.

D. Spatial Attraction

All users tend to keep their positions, but the battery depleting users are willing to move for charging a unit energy amout P_u with the SA distance $r_a (\leq \hat{r}_a)$. Specifically, assuming B_2's broadcast their locations, a user is spatially attracted toward its nearest B_2 if the following two SA conditions hold: (i) $L \in \{L_0, L_1\}$ and (ii) $r_a \leq \hat{r}_a$. The former indicates users are battery depleting (or U_ℓ), and the latter represents SA distance should be no greater than the users' maximum feasible SA distance. The required amount of energy to receive the B_2 location information is assumed to be negligible; so that even L_0 users can successfully receive it. Such SA affects user locations, and thus results in user mobility model specified by the following two phases. For each unity time slot, they occur in order.

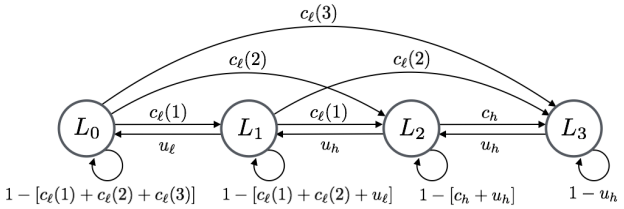

Fig. 2. Four-level residual battery energy Markov chain where the state L_i corresponds to the maximum i number of information receptions.

1. *(Uniform Distribution):* Users are uniformly distributed.
2. *(Spatial Attraction):* SA users move toward their nearest B_2 through the shortest paths until reaching B_2's charging rim providing P_u (see yellow thick circle in Fig. 1); non-SA users keep their locations.

III. SAN Rate Coverage Maximization

In this section we focus on WPT charging power P_{tc}, as well as its corresponding r_c, that maximizes average rate coverage $\mathcal{R}$ in an SAN, the probability that a typical user's average downlink rate exceeds a target threshold θ. We rigorously specify the definition as

$$\mathcal{R} := \mathsf{E}_{\Phi_k}\left[\frac{u}{N_k + 1} \mathbb{P}\big(\log[1 + \mathsf{SIR}_k] > \frac{\theta}{W} \big) \right] \tag{4}$$

where N_k represents the number of users in a B_k associated with a typical user.

A. Association Probability

In SAN, a user is associated with a BS based on its residual energy and the received power strength.

Lemma 1. The probability $\mathcal{A}_k^h$ (or $\mathcal{A}_k^\ell$) that U_h (or U_ℓ) associates with B_k is given as

$$\mathcal{A}_k^h = \left[{\lambda_k}^{-1} \sum_{i=1}^{2} \lambda_i \left(\frac{P_i}{P_k} \right)^{\frac{2}{\alpha}} \right]^{-1}, \tag{6}$$

$$\mathcal{A}_k^\ell = (-1)^k \left(\mathcal{A}_2^h e^{-\pi \frac{\lambda_2}{\mathcal{A}_2^h} {r_s}^2} - e^{-\pi \lambda_2 {r_s}^2} \right) + (k-1) \tag{7}$$

where $r_s = r_c + \hat{r}_a$.

Proof. See Appendix-A. ■

Such a BS association changes the association distance as well as the number of associated users. They are derived by utilizing Lemma 1, to produce the rate coverage.

B. Rate Coverage and Its Optimal Charging Power

To state our main result, the rate coverage, let $\mathbf{q}$ denote the steady-state probability vector of each residual battery energy level, $\mathbf{q} = [q_0, q_1, q_2, q_3]$, whose states and transition probabilities are shown as a Markov chain in Fig. 2. SAN rate coverage $\mathcal{R}$ is represented in the following proposition.

Proposition 1. Rate coverage in an SAN is given as

$$\mathcal{R} = \sum_{k=1}^{2} \left(\sum_{n\geq 1} \frac{\mathbb{P}(N_k = n)}{n+1} \left[P_H \mathcal{A}_k^h \mathcal{R}_k^h + P_L \mathcal{A}_k^\ell \mathcal{R}_k^\ell \right] \right). \quad (8)$$

The residual battery energy dependent information reception probabilities $P_H = (q_2 + q_3)u_h$ and $P_L = q_1 u_\ell$ for q_1, q_2, and q_3, which are obtained by solving $\mathbf{qT} = \mathbf{q}$ where

$$\mathbf{T} = \begin{bmatrix} 1-\sum_{i=1}^{3} c_\ell(i) & c_\ell(1) & c_\ell(2) & c_\ell(3) \\ u_\ell & 1-u_\ell-\sum_{i=1}^{2} c_\ell(i) & c_\ell(1) & c_\ell(2) \\ 0 & u_\ell & 1-u_\ell-c_\ell(1) & c_\ell(1) \\ 0 & 0 & u_h & 1-u_h \end{bmatrix},$$

$$c_\ell(1) = e^{-\pi\lambda_2 2^{-\frac{2}{\beta}} r_c{}^2} - e^{\pi\lambda_2 (r_c+\hat{r}_a)^2},$$
$$c_\ell(2) = e^{-\pi\lambda_2 3^{-\frac{2}{\beta}} r_c{}^2} - e^{-\pi\lambda_2 2^{-\frac{2}{\beta}} r_c{}^2},$$
$$c_\ell(3) = 1 - e^{-\pi\lambda_2 3^{-\frac{2}{\beta}} r_c{}^2}, \text{ and}$$
$$c_h = 1 - e^{-\pi\lambda_2 r_c{}^2}.$$

The distribution of B_k associated user number is $\mathbb{P}(N_k{=}n) = \sum_{m=0}^{n} \mathbb{P}\big(N_k^h{=}n{-}m\big)\mathbb{P}\big(N_k^\ell{=}m\big)$ where

$$\mathbb{P}\Big(N_k^h{=}n\Big) = \frac{3.5^{3.5}\Gamma(n{+}4.5)}{n!\Gamma(3.5)} \left(\frac{\lambda_u P_H \mathcal{A}_k^h}{\lambda_k}\right)^n \left(3.5{+}\frac{\lambda_u P_H \mathcal{A}_k^h}{\lambda_k}\right)^{-(n+4.5)},$$
$$\mathbb{P}\Big(N_k^\ell{=}n\Big) = \frac{3.5^{3.5}\Gamma(n{+}4.5)}{n!\Gamma(3.5)} \left(\frac{\lambda_u P_L \mathcal{A}_k^\ell}{\lambda_k}\right)^n \left(3.5{+}\frac{\lambda_u P_L \mathcal{A}_k^\ell}{\lambda_k}\right)^{-(n+4.5)}.$$

Given residual battery energy and associations, rate coverages are in (5) at the bottom of the page.

Proof. See Appendix-B. ■

It is worth noting that SAN rate coverage does not monotonically increase with the charging power P_{tc} as shown in Fig. 3(b). The reason is explained by the following two perspectives.

1) *The trade-off between load balanging and spectral efficiency gains:* Increasing P_{tc} (or r_c) attracts more users toward small cell areas for load balanging while reducing the spectral efficiency improvement that can be achieved by shortening the distance to BS.
2) *SA motivation:* Too small power P_{tc} motivates few SA that cannot sufficiently operate an SAN so as to provide a rate coverage improvement. Charging too much power, in contrast, retains mobile users' residual energy enough and may lose their SA motivations, decreasing the improvements in both load balanging and spectral efficiency.

This makes us turn our attention to derive the optimal charging power P_{tc}^* maximizing rate coverage. This derivation is not straightforward due to the user safety condition. The received charging power density of a user should not exceed the maximum safe power density η [17], delimiting the feasible range of P_{tc}^*. Furthermore, the maximum feasible amount of P_{tc}^*, as well as its corresponding distance r_c, is also restricted by B_2 Voronoi cell inscribed circle radius ν; otherwise, SA does not always increase spectral efficiency and load balancing, which may degrade rate coverage. We collectively consider such trade-off and constrains on P_{tc}, and yield its optimal value.

Proposition 2. Assuming the load at each BS is equal to its mean to simplify SAN rate coverage, the optimal charging power P_{tc}^* is given as

$$P_{\text{tc}}^* = \min\left\{ \underset{P_{\text{tc}}}{\text{argmax}} \sum_{k=1}^{2} \frac{P_H \mathcal{A}_k^h \mathcal{R}_k^h + P_L \mathcal{A}_k^\ell \mathcal{R}_k^\ell}{1 + 1.28\frac{\lambda_u}{\lambda_k}\left(P_H \mathcal{A}_k^h + P_L \mathcal{A}_k^\ell\right)}, \hat{P}_{\text{tc}}^\eta, \hat{P}_{\text{tc}}^\nu \right\} \quad (9)$$

$$\mathcal{R}_k^h = \frac{1}{1+\rho_{(\theta,M)}}$$

$$\mathcal{R}_1^\ell = \frac{e^{-\pi\lambda_2\left(P_{tc}{}^{\frac{1}{\beta}}+\hat{r}_a\right)^2 \mathrm{L}_2(\theta)}}{\mathrm{L}_1(\theta)\mathcal{A}_1^\ell} + \frac{e^{-\pi\lambda_2\left(P_{tc}{}^{\frac{1}{\beta}}+\hat{r}_a\right)^2}}{\mathcal{A}_1^\ell} \int_0^M r e^{-\pi\lambda_1 r^2\left[1+\rho_{(\theta,M)}+\lambda\rho_{(\theta,r)}\right]} dr$$

$$\mathcal{R}_2^\ell = \frac{e^{-\pi\lambda_2\left(P_{tc}{}^{\frac{1}{\beta}}+\hat{r}_a\right)^2 \mathrm{L}_2(\theta)}}{\mathrm{L}_2(\theta)^{-1}\mathcal{A}_2^\ell} + \frac{\mathcal{A}_2^h - \mathcal{A}_2^h e^{-\pi\lambda_2 P_{tc}{}^{\frac{2}{\beta}}\left[1+\frac{\rho(\theta,M)}{\mathcal{A}_2^h}\right]}}{\mathcal{A}_2^\ell\mathcal{A}_2^h + \mathcal{A}_2^\ell\rho_{(\theta,M)}} + \frac{e^{-\pi\lambda_2 P_{tc}{}^{\frac{2}{\beta}}\left[1+\frac{\rho(\theta,M)}{\mathcal{A}_2^h}\right]} - e^{-\pi\lambda_2 P_{tc}{}^{\frac{2}{\beta}}\left[\frac{\rho(\theta,M)}{\mathcal{A}_2^h} + \left(1+\frac{\hat{r}_a}{P_{tc}{}^{\frac{1}{\beta}}}\right)^2\right]}}{\mathcal{A}_2^\ell}$$

$$\rho_{(\theta,x)} = (e^{\frac{\theta}{W}}-1)^{\frac{2}{\alpha}} \int_{\left(\frac{M}{x}\right)^2 (e^{\frac{\theta}{W}}-1)^{-\frac{2}{\alpha}}}^{\infty} \left(1+u^{\frac{\alpha}{2}}\right)^{-1} du, \mathrm{L}_k(\theta) = \frac{1+\rho_{(\theta,M)}}{\mathcal{A}_k^h}, M = \left(P_{tc}{}^{\frac{1}{\beta}}+\hat{r}_a\right)\left(\frac{P_1}{P_2}\right)^{\frac{1}{\alpha}}, \lambda = \frac{\lambda_2}{\lambda_1}\left(\frac{P_2}{P_1}\right)^{\frac{2}{\alpha}} \quad (5)$$

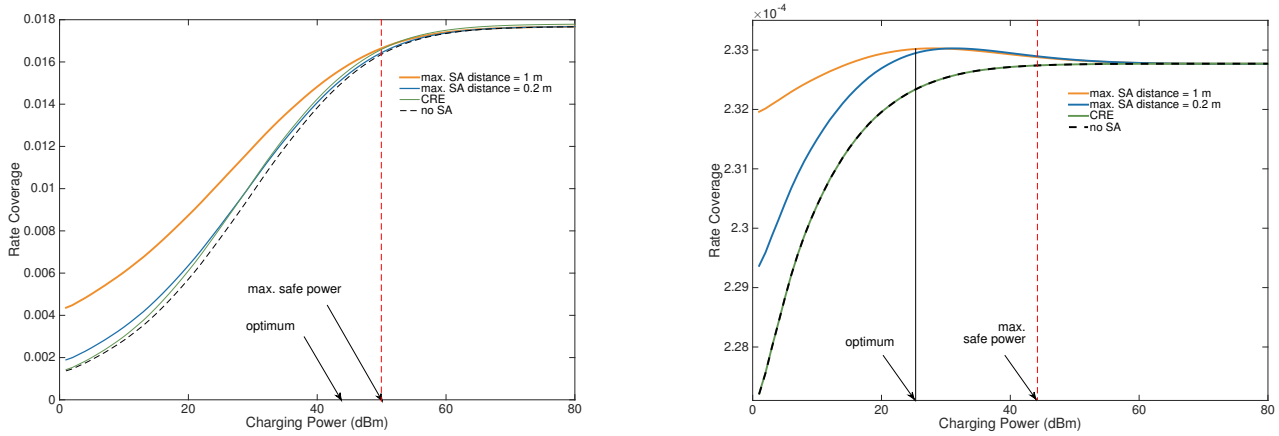

(a) For $\lambda_u = 2\times10^4$ users/km^2, $\lambda_2 = 3\times10^2$ BSs/km^2

(b) For $\lambda_u = 1\times10^7$ users/km^2, $\lambda_2 = 3\times10^3$ BSs/km^2

Fig. 3. Rate coverage in an SAN ($\lambda_1 = 10$ BSs/km^2, $P_1 = 43$ dBm, $P_2 = 23$ dBm, $W = 10$ MHz, $\theta = 1$ Mbps, $\alpha = 4$, $\beta = 5$, $\eta = 10$ W/m^2, $G_m = 20$ dBi, $G_s = -6.5$ dBi [20]).

where

$$\hat{P}_{\text{tc}}^{\eta} = \frac{2G_m\lambda_2 P_{\text{tc}}}{\tan^2(\frac{t_m}{2})}\left[1 - e^{-\lambda_2\pi} - \lambda_2\pi\text{Ei}(-\lambda_2\pi)\right], \text{ and}$$

$$\hat{P}_{\text{tc}}^{\nu} = \frac{1}{G_m}\left(16\lambda_2 + 4\left[1 + \left(\frac{P_1}{P_2}\right)^{\frac{1}{\alpha}}\right]^2\lambda_1\right)^{-\frac{\beta}{2}} \tag{10}$$

where t_m denotes a beam width and $\text{Ei}(x)$ an exponential integral function.

Proof. Appendix-C ■

Although an optimal charging power P_{tc}^* derivation is not possible in a closed form, it can be discovered through a linear search utilizing the above proposition, which is easily accessible compared to running an exhaustive simulation. Furthermore, to get a closed form optimal value, we consider an asymptotic case where the user density is much higher than BSs'.

Corollary 1. For $\lambda_u \gg \lambda_k$, P_{tc}^* is given as below.

- *When* $\lambda_1 \ll \lambda_2$,

$$P_{\text{tc}}^* \approx \frac{1}{G_m}\left[\left(\frac{1+\rho_{(\theta,T)}}{6\pi\left[\lambda_1\left(\frac{P_1}{P_2}\right)^{\frac{2}{\alpha}} + \lambda_2\right]} - \frac{\hat{r}_a^2}{12}\right)^{\frac{1}{2}} - \frac{1}{2}\hat{r}_a\right]^{\beta} \tag{11}$$

- *When* $\lambda_1 \geq \lambda_2$,

$$P_{\text{tc}}^* \approx \frac{1}{G_m}\left[\left(27\pi\rho_{(\theta,T)}\left[\lambda_1\left(\frac{P_1}{P_2}\right)^{\frac{2}{\alpha}} + \lambda_2\right]\right)^{-\frac{1}{2}} - \frac{3}{2}\hat{r}_a\right]^{\beta}. \tag{12}$$

Proof. Appendix-D ■

The result provides a charging power control guideline in an SAN as follows. For low small cell density λ_2 and/or the SA distance $\hat{r}_a$, the SAN is likely to suffer from macro cell traffic congestion, requiring to attract more users to small cells for load balanging. In such a scenario, P_{tc}^* should be increased, and vice versa for the opposite situation. For a large threshold θ, spectral efficiency dominates the rate coverage, and thus P_{tc}^* should be decreased to shorten the association distances, increasing spectral efficiency.

Fig. 3 illustrates the SAN rate coverage that is superior to the case with no SA, and the improvement increases along with SA motivation (or maximum SA distance $\hat{r}_a$). Moreover, it captures the proposed network outperforms a network with CRE that is beneficial to load balancing yet is harmful to spectral efficiency [13], [14]. Specifically, when it comes to load balancing, CRE resorts to decreasing the received power from an associated BS. In an SAN, on the contrary, its load balancing coincidentally shortens user association distance, and therefore also increases the received power from an associated BS, leading to the further improvement in rate coverage than CRE. It is worth mentioning that if users are willing to move at least 20 cm for battery charging, an SAN become superior in rate coverage to the network with CRE. Though, SAN may achieve lower rate coverage than CRE if users are unlikely to be attracted, as shown in Fig. 3(a).

Regarding a user safety requirement, the optimal charging power may exceed the maximum safe charging power (red dotted lines). However, such a situation can be detoured via high user density or deploying more small cells as in Fig. 3(b).

Fig. 4 depicts the maximized SAN rate coverage monotonically increases with small cell BS density. This relentless improvement is expected to be different from the case with

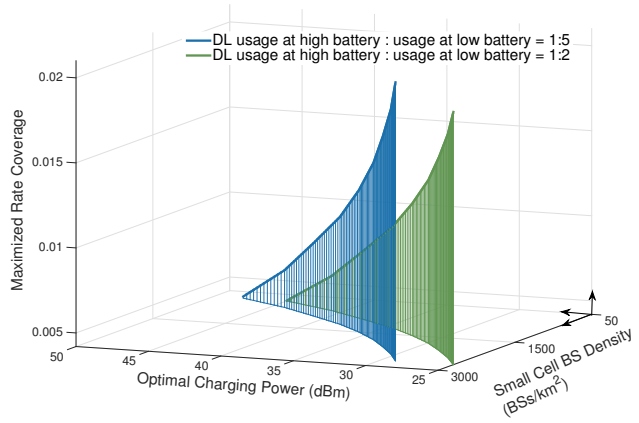

Fig. 4. Maximized rate coverage and optimal charging power with respect to the λ_2 and DL usage ratio $\frac{u_h}{u_\ell}$ (λ_1=10 BSs/km^2, λ_u=1×10^4 users/km^2, P_1=43 dBm, P_2=23 dBm, W=10 MHz, θ=1 Mbps, α=4, β=5, $\hat{r}_a$= 2 m, G_m=10 dBi, G_s=−7.4 dBi [20]).

CRE whose improvement is saturated for high small cell BS density where load balancing is not much needed (see the convergence of dotted black and solid green lines in Fig. 3(b)). SAN can increase rate coverage via its spectral efficiency improvement even viable in such an environment. Focusing on the exponentially decreasing optimal charging power along with small cell BS density, deploying small cells can be a viable solution for ever-growing rate coverage while abiding by a safety requirement.

In addition, the proposed SAN can improve much more rate coverage when DL traffic usage ratio of low-to-high battery users is large, i.e. when users are more sensitive to their residual energy. This represents that SAN effects well along with a growth of booming wireless communication services that require large battery consumptions.

IV. Conclusion

In this paper we have analyzed an SAN that spatially attracts battery depleting users by means of providing WPT battery charging. The result sheds light on WPT charging power control in order to maximize rate coverage of the SAN. Our analytic result reveals that charging power increase as much as possible does not guarantees the maximum rate coverage, and thus its optimization is required. Such an optimal charging power is derived in a closed form, and its corresponding design guideline is presented for different network deployment, wireless channel environment, and a user safety requirement.

The weakness of this study is its one-sided focusing on a downlink scenario. SA has a potential to further improve uplink rate coverage by its shrinking association distances. In such a scenario, the uplink optimal charging power may not be in accordance with the downlink optimal charging power. Further extension to this work therefore should involve their joint optimization problem. Another interesting avenue for future work is a network economic analysis on the SAN. In a similar way to [21], the SAN rate coverage optimization will jointly incorporate BS density and spectrum amount for communications, also combined with such values for WPT, providing a network operator's SAN deployment guideline.

Appendix

A. Proof of Lemma 1

For U_h, the association probability $\mathcal{A}_k^h$ is directly derived by using Lemma 1 in [19]. For U_ℓ, the association probability $\mathcal{A}_k^\ell$ should incorporate the SA impact. Let r_k denote the distance between a typical U_ℓ and his nearest B_k. Now that a U_ℓ is attracted toward the nearest B_2 if $r_2<r_s$, $\mathcal{A}_1^\ell$ is given as

$$\begin{aligned}\mathcal{A}_1^\ell &= \mathbb{P}(U_\ell \to B_1 \text{ and } r_2 \geq r_s)\\ &= \mathbb{P}\left(P_1 {r_1}^{-\alpha} \geq P_2 {r_2}^{-\alpha} \text{ and } r_2 \geq r_s\right)\\ &\overset{(a)}{=} 2\pi\lambda_1 \int_{r_s\left(\frac{P_1}{P_2}\right)^{\frac{1}{\alpha}}}^{\infty} r e^{-\pi r^2 \sum_{i=1}^{2}\lambda_i \left(\frac{P_i}{P_1}\right)^{\frac{2}{\alpha}}} dr\\ &\quad + 2\pi\lambda_1 e^{-\pi\lambda_2 {r_s}^2} \int_0^{r_s\left(\frac{P_1}{P_2}\right)^{\frac{1}{\alpha}}} r e^{-\pi\lambda_1 r^2} dr \end{aligned} \tag{13}$$

where (a) follows from the nearest neighbor distance distribution [15]. Similarly, $\mathcal{A}_2^\ell$ is given as

$$\begin{aligned}\mathcal{A}_2^\ell &= \mathbb{P}(U_\ell \to B_2 \text{ or } r_2 < r_s)\\ &= \mathbb{P}\left(P_2 {r_2}^{-\alpha} \leq P_1 {r_1}^{-\alpha},\ r_2 \geq r_s\right) + \mathbb{P}(r_2 < r_s)\\ &= 2\pi\lambda_2 \int_{r_s}^{\infty} r e^{-\pi\left(\sum_{i=2}^{2}\lambda_i \frac{P_i}{P_2}^{2/\alpha} + \lambda_2\right) r^2} dr + 1 - e^{-\pi\lambda_2 {r_s}^2} \end{aligned} \tag{14}$$

that finalizes the proof. ■

B. Proof of Proposition 1

The desired result comes from the following four parts.

1) Residual Energy Dependent Information Reception Probabilities P_H and P_L: Let $c_\ell(i)$ denote the probability that U_ℓ is capable of additional i times information receptions thanks to WPT battery charging. Its calculation is followed by the fact that U_ℓ can receive i times information receptions thanks to battery charging if $2^{-\frac{2}{\beta}} r_c < r_2 \leq r_c + \hat{r}_a$ for i=1 and if $(i+2)^{-\frac{1}{\beta}} r_c < r_2 \leq (i+1)^{-\frac{1}{\beta}} r_c$ for i=2,3. Let c_h denote the battery charging probability of U_h. The event of c_h is identical to the event that U_h is located with the distance closer than r_c from the nearest B_2. Applying void probabilities [15] to their spatial regions of $c_\ell(i)$ and c_h yield the calculations.

2) BS Association Distance Distribution: Now that an SA user goes toward the nearest B_2, the distance between them diminishes. For the SA affected association distance for U_ℓ, its complementary cumulative distribution function (CCDF) is

$$\mathbb{P}(r_k>r|U_\ell\to B_k)=\frac{\mathbb{P}(r_k>r \text{ and } U_\ell\to B_k)}{\mathcal{A}_k^\ell} \tag{15}$$

where $U\to B_k$ denotes an event that a user U associates with a B_k. For the probability density function (PDF) $f_{r_1}^\ell(r)$, calculating the numerator in CCDF requires a simple modification of (14) in the proof of Lemma 1. For $f_{r_2}^\ell(r)$, the numerator calculation is divided into two cases: (i) if $r_c\le r_2<r_s$, an U_ℓ is located at a distance of r_c from B_2; (ii) if $r_2<r_c$, r_c is restricted to the B_2 cell, making the calculation become the void probability [15] of a ball with radius r_2. Applying Lemma 1 and differentiating CCDF derive $f_{r_k}^\ell(r)$ as below.

$$f_{r_1}^\ell(r)=\begin{cases}\frac{2\pi\lambda_1}{\mathcal{A}_1^\ell}re^{-\pi\sum_{i=1}^2\lambda_i\left(\frac{P_i}{P_1}\right)^{\frac{2}{\alpha}}r^2} & \text{if } r<r_s\left(\frac{P_1}{P_2}\right)^{\frac{1}{\alpha}}\\ \frac{2\pi\lambda_1}{\mathcal{A}_1^\ell}e^{-\pi\lambda_2{r_s}^2}re^{-\pi\lambda_1r^2} & \text{otherwise}\end{cases}, \tag{16}$$

$$f_{r_2}^\ell(r)=\begin{cases}\frac{2\pi\lambda_2}{\mathcal{A}_2^\ell}re^{-\pi\lambda_2r^2} & \text{if } r<r_c\\ \delta_{r_c}\frac{e^{-\pi\lambda_2{r_c}^2}-e^{-\pi\lambda_2{r_s}^2}}{\mathcal{A}_2^\ell} & \text{if } r_c\le r<r_s\\ \frac{2\pi\lambda_2}{\mathcal{A}_2^\ell}re^{-\pi\sum_{i=1}^2\lambda_i\left(\frac{P_i}{P_2}\right)^{\frac{2}{\alpha}}r^2} & \text{otherwise}\end{cases} \tag{17}$$

where δ_{r_c} is a Dirac delta function yielding 1 for $r=r_c$, otherwise 0. The PDF $f_{r_k}^h(r)$ for U_h is provided by Lemma 4 in [14] as $\frac{2\pi\lambda_k}{\mathcal{A}_k^h}re^{-\pi r^2\sum_{i=1}^2\lambda_i\left(\frac{P_i}{P_k}\right)^{\frac{2}{\alpha}}}$.

3) Distribution of B_k Associated User Number: The probability mass function of the user number N_k excluding a typical user associated with a B_k is derived by using Lemma 1 and Corollary 1 in [14].

4) Rate Coverages Conditioned on Residual Energy and an Association $\mathcal{R}_k^h$ and $\mathcal{R}_k^\ell$: Applying Theorem 1 in [14] with the preceding results and Lemma 1 enables to calculate the rate coverages. When it comes to averaging interferer locations, it is worth noting that small cell interferer distances at a B_1 associated typical U_ℓ range from r_s to ∞ if $r_1<M$; otherwise, the interferer distances range from 0 to ∞. ■

C. Proof of Proposition 2

For analytical tractability, we approximate the number of the k-th tier associated users as its average value as below [14].

$$\mathsf{E}[N_k]=\frac{1.28\lambda_u}{\lambda_k}\left(P_H\mathcal{A}_k^h+P_L\mathcal{A}_k^\ell\right). \tag{18}$$

The feasible range of charging power is restricted by a safety requirement. Since a user recieves the charging power with main lobe gain from his associated B_2 and received power from other B_2's is assumed to be negligibly small, the average received power density $\dot{P}_{rc}$ is represented as

$$\begin{aligned}\dot{P}_{\text{rc}}&\overset{(a)}{=}\mathsf{E}_{\Phi_2}\left[\frac{G_mP_{\text{tc}}}{\pi\tan^2(\frac{t_m}{2})\max\left\{\left|B_2^{(0)}\right|,1\right\}^2}\right]\\&=\frac{2G_m\lambda_2P_{\text{tc}}}{\tan^2(\frac{t_m}{2})}\left(\int_0^1re^{-\lambda_2\pi r^2}dr+\int_1^\infty\frac{re^{-\pi\lambda_2r^2}}{r^2}dr\right)\\&=\frac{2G_m\lambda_2P_{\text{tc}}}{\tan^2(\frac{t_m}{2})}\left[1-e^{-\lambda_2\pi}-\lambda_2\pi\text{Ei}(-\lambda_2\pi)\right]\end{aligned}$$

where (a) follows from surface area of power transmission in main lobe [20], t_m denotes a beam width, and $\text{Ei}(x)$ an exponential integral function.

Applying the safety requirement $\dot{P}_{rc}\le\frac{\eta}{P_u}$ results in $\hat{P}_{tc}^\eta$. Another factor delimiting the feasible range of charging power is Voronoi cell area, i.e. the maximum charging distance r_c is no larger than the inradius of a B_2 cell area ν. To simplify our exposition, we approximate ν as its expected value $\mathsf{E}[\nu]$ calculated by using [18].

$$\mathsf{E}[\nu]=(16\lambda_2+4[1+(P_1/P_2)^{1/\alpha}]^2\lambda_1)^{-1/2}. \tag{19}$$

Applying the maximum charging range requirement $\hat{P}_{tc}^\nu=\frac{\mathsf{E}[\nu]^\beta}{G_m}$ completes the proof. ■

D. Proof of Corollary 1

When $\lambda_u\gg\lambda_k$, $\mathcal{R}\approx P_L\mathcal{A}_2^\ell(\mathcal{R}_2^\ell-\mathcal{R}_2^h)(P_H\mathcal{A}_2^h+P_L\mathcal{A}_2^\ell)^{-1}$. Applying Taylor expansion with a linear interpolation simplifies $\mathcal{R}$ as $\pi\frac{\lambda_2}{\mathcal{A}_2^h}\rho_{(\theta,T)}\left(4\hat{r}_a^3r_c+6\hat{r}_a^2{r_c}^2+4\hat{r}_a{r_c}^3+\hat{r}_a\right)-\left(1+\rho_{(\theta,T)}\right)\left(2\hat{r}_ar_c+\hat{r}_a^2\right)$ for $\lambda_1\ll\lambda_2$. In a similar way, the approximation of $\mathcal{R}$ for $\lambda_1\ge\lambda_2$ becomes $\pi\lambda_2\left(2\hat{r}_ar_c+\hat{r}_a^2\right)-\pi^2{\lambda_2}^2\frac{\rho_{(\theta,T)}}{\mathcal{A}_2^h}\left(2\hat{r}_a{r_c}^3+\hat{r}_a^2{r_c}^2\right)$. Differentiating the approximated $\mathcal{R}$ with respect to r_c yields the optimal charging power. ■

ACKNOWLEDGEMENT

This work was supported by Institute for Information & communications Technology Promotion (IITP) grant funded by the Korea government (MSIP) (No.B0126-16-1017, Spectrum Sensing and Future Radio Communication Platforms).

REFERENCES

[1] V. Pauli, J. D. Naranjo, and E. Seidel, "Heterogeneous lte networks and inter-cell interference coordination," Nomor Research GmbH, December 2010.

[2] J.-M. Moon, J. Jung, S. Lee, A. Nigam, S. Ryoo, "On the trade-off between handover failure and small cell utilization in heterogeneous networks," in *Proc. IEEE International Conference on Communication Workshop (ICCW),* London, United Kingdom, Jun. 2015

[3] J.D. Power, "Battery life: Is that all there is?," Apr. 2012, *available at: http://tiny.cc/jdpower*

[4] N. Friedman, "Wireless charging stations means even Starbuck haters will soon be ordering frappuccinos," Jul. 2014, *available at: http://tiny.cc/sbwpt*

[5] Intel, "Intel survey: tech norms for travelers," *Intel News Release*, Jun. 2012.

[6] J.A. Paradiso and T. Starnet, "Energy scavenging for mobile and wireless electronics," *IEEE Pervasive Computing*, vol. 4, no. 1, pp. 18–27, 2005.

[7] Alan F., "McDonald's is bringing Qi wireless charging to selected U.K. restaurants," Jan. 2015, *available at: http://tiny.cc/mcwpt*

[8] K. Huang and X. Zhou, "Cutting last wires for mobile communications by microwave power transfer," *IEEE Commun. Mag.,* vol. 53, no. 6, pp. 86–93, 2015.

[9] A. Kurs, R. Moffatt, and M. Soljacic, "Simultaneous mid-range power transfer to multiple devices," *Appl. Phys. Lett.*, vol. 96, no. 4, 2010.

[10] TechCrunch, "Cota by Ossia aims to drive a wireless power revolution and change how we think about charging," Sep. 2013, *available at: http://tiny.cc/tchcrunch*

[11] S.-W. Ko, S. M. Yu, and S.-L. Kim., "The capacity of energy-constrained mobile networks with wireless power transfer," *IEEE Commun. Lett.*, vol. 17, no. 3, pp. 529–532, 2013.

[12] K. Huang and V. K. N. Lau, "Enable wireless power transfer in cellular network: architecture, modeling and deployment," *IEEE Trans. Wireless Commun.*, vol. 13, no. 2, pp. 902–912, 2014.

[13] A. Damnjanovic et al., "A survey on 3GPP heterogeneous networks," *IEEE Wireless Commun. Mag.*, vol. 18, no. 3, pp. 10–21, 2011.

[14] S. Singh, H. S. Dhillon, and J.G. Andrews, "Offloading in heterogeneous networks: Modeling, analysis, and design insights," *IEEE Trans. Wireless Commun.*, vol. 12, no. 5, pp. 2484–2497, 2013.

[15] D. Stoyan, W. S. Kendall, and J. Mecke, *Stochastic Geometry and Its Applications*, Wiley, 2nd ed., 1995.

[16] D. N. C. Tse and P. Viswanath *Fundamentals of Wireless Communications*, Cambridge University Press, 2005.

[17] K. R. Foster, "A world awash with wireless devices: Radio-frequency exposure issues," *IEEE Microwave Mag.*, vol. 14, no. 2, pp. 73–84, 2013.

[18] P. Calka, "The distributions of the smallest disks containing the Poisson-Voronoi typical cell and the Crofton cell in the plane," *Adv. in Appl. Prob.*, 702–717, 2002.

[19] H.-S. Jo, Y. J. Sang, P. Xia, and J. G. Andrews, "Heterogeneous cellular networks with flexible cell association: A comprehensive downlink SINR analysis," *IEEE Trans. Wireless Commun."*, vol. 11, no. 10, pp. 3484–3495, 2012.

[20] R. Ramanathan, "On the performance of ad hoc networks with beamforming antennas." in *Proc. ACM international symposium on Mobile ad hoc networking & computing (MobiHoc)*, Long Beach, United States, Oct. 2011.

[21] J. Park, S.-L. Kim, and J. Zander, "Asymptotic Behavior of Ultra-Dense Cellular Networks and Its Economic Impacts," in *Proc. IEEE Global Communications Conference (GLOBECOM)*, Austin, United States, Dec. 2014.